IJMEI

International Journal of Mining & Environmental Issues,
Vol. 1, No.1, 2010.

GIS modelling for Au-Pb-Zn potential mapping in Torud-Chah Shirin area- Iran

M. Ziaii[1*], A. Abedi[1], M. Ziaei[1], A. Kamkar Rouhani[1], A. Zendahdel[1]

1. Faculty of Mining, Petroleum and Geophysics, Shahrood University of Technology; Shahrood, Iran

Received 15 April 2009; accepted 23 February 1010
*e-mail: Mziaii@ shahroodut.ac.ir

Abstract

One of the major strengths of a Geographic Information System (GIS) in geosciences is the ability to integrate and combine multiple layers into mineral potential maps showing areas which are favorable for mineral exploration. These capabilities make GIS an extremely useful tool for mineral exploration. Several spatial modeling techniques can be employed to produce potential maps. However, these methods can be divided into knowledge - and data- driven techniques. The goal of this study is to use GIS in mapping gold deposit potentials in Torud-Chah Shiran area. After collecting relevant exploration data and defining appropriate exploration model for the mineralization zone, several layers including proved mineralization map, geological map, remote sensing derived, alteration map, geochemical and aeromagnetic maps were imported in to GIS environment. For integrated exploration modeling, two methods were used: fuzzy logic and weight of evidence methods. Finally, the results of the two methods were compared. The result of each method had statistical problems but these problems were alleviated using the map of differences that was in a good agreement with reality.

Keywords: *Fuzzy logic method, Weight of evidence method, GIS, Torud-Chah Shiran area*.

1. Introduction

Models for spatial data analysis in GIS are simplified representations of natural phenomena. The rational for this simplification is related to the complexity of the natural processes, and the limitations of the mathematical techniques used for representing these phenomena. The consequence is a reduction on our explanatory capability, since the simplified relationships used in the model may cause misleading or incomplete conclusions. The formation of a mineral deposit is a good example of such a situation. Since the complexity of the physical and chemical conditions involved in the mineralization processes cannot be adequately mathematically expressed, the success of a prospecting model depends mainly on empirical relations (deposit models). These models consist of a large number of known deposits, considered to be sufficiently in terms of their characteristics, which are used as guides (description models) for prospecting similar deposits. Therefore, in GIS-based studies, “deposit model” plays an important role both in the selection and derivation of the data that will be considered as evidence, as well as in the definition of the weights assigned to the evidence. To become an effective tool for geological exploration, a prospecting model must be supported by appropriate geological basis and adequate mathematical support. Following these principles, several investigators used prospecting model as auxiliary tools for mineral prospecting [1-4].

Interpretation of aeromagnetic, Landsat TM, geological and mineral occurrence data are used to recognize a combination of mapped geological features, spectral characteristics, and magnetic signatures that could be associated with epithermal gold, arsenic, antimony, and base metal deposits near Takab (NW Iran). Four binary maps representing diagnostic deposit recognition criteria were combined in a weights-of-evidence model, which uses the spatial distribution of 19 known mineral occurrences to calculate a final map of further gold and base metal potential in the Takab area [5].

As a contribution to this theme, the present study compares the results of different methods of spatial analysis. These methods involved fuzzy logic and weights of evidence methods to predict potential area for gold and base metal occurrences in the Torud-Chah Shiran metallogenic zone in Iran (Figure 1).

Figure 1. Location of Torud-Chah Shiran mineral field in the Alborz magmatic belt of northern Iran.

The fuzzy logic method is one of knowledge–driven methods while weight of evidence is considered to be in the category of data-driven methods. The techniques of spatial inference were applied according to a prospecting model based on four diagnostic criteria which are presence of particular geological units, presence of structural features, presence of geophysical anomalies, and presence of geochemical anomalies obtained from stream sediments data. Twenty previously recognized mineral occurrences were used as a guide to estimate the performance of the obtained results.

2. Geological description of the study area

Torud-Chah Shirin range mainly consists of igneous rocks of Tertiary age, although there are also scattered outcrops of metamorphosed Paleozoic and Mesozoic rocks. Structural patterns are controlled by two principal strike-slip faults, Anjilow in the north and Torud in the south, both with northeast trends as shown in Figure 2 [6].

The Torud-Chah Shiran range, which lies in the central to eastern portion of the Alborz mountain system, is the largest known gold and base metal province of Iran [7,8]. In this province, the northern Iran region hosts five gold and base metal deposits, i.e., Gandy (Au-Ag-Pb-Zn), Abolhassani (Pb-Zn-Ag-Au), Cheshmeh Hafez (Pb-Zn), Chalu(Cu), Chahmosa (Cu), pousideh (Cu), Baghu and Arghash(Au-Sb) deposit. Other types of deposits in this range include placer gold, an underground mine for turquoise at Baghu, skarn deposits, and Pb-Zn deposits in carbonate rocks.

The Gandy and Abolhassani areas are about 3 km apart, and each contains a small abandoned Pb-Zn mine. Mineralisation at Gandy occurs in quartz sulfide veins and breccias and is accompanied by alteration halos of quartz, illite, and calcite. Mineralisation in the Abolhassani veins occurred in three main stages. The first two stages, which are economically important, contain similar mineral assemblages, including quartz, calcite, barite, galena, sphalerite, pyrite, and chalocopyrite, whereas the final stage is dominated by quartz and calcite. The mineralogy of ore, gangue, and alteration products, combined with fluid inclusion data from both areas, indicate that these are intermediate-sulfidation epithermal veins that share characteristics with those of major districts in Mexico, western United State, Peru, and elsewhere. The presence of geochemical anomalies and many ore showings abandoned mines (Figure 2) with similar epithermal characteristics suggests that the Torud-Chah Shiran range is prospective for high-grade gold veins and base metal epithermal deposits [8,9].

3. Datasets collected for the present study

3.1. Geological map

Data sets used in the current paper are, a geological map and lineaments map digitized from the 100,000 scale geological map of the area published by Geological Survey of Iran, figure 2. Peak magmatic activity has occurred from middle to possibly late Eocene and has been divided into three stages, from oldest to youngest as follows: (1) explosive volcanic activity represented by rhyolitic to rhyodacitic tuffs and locally andesitic lava flows, with subordinate marls, tuffaceous marlstones, and sandstones; (2) lava flows and pyroelastic rocks of andesite, trachyandesite, and basaltic andesite composition; and (3) subordinate dacitic-rhyodacitic rocks and hypabyssal intrusive rocks.

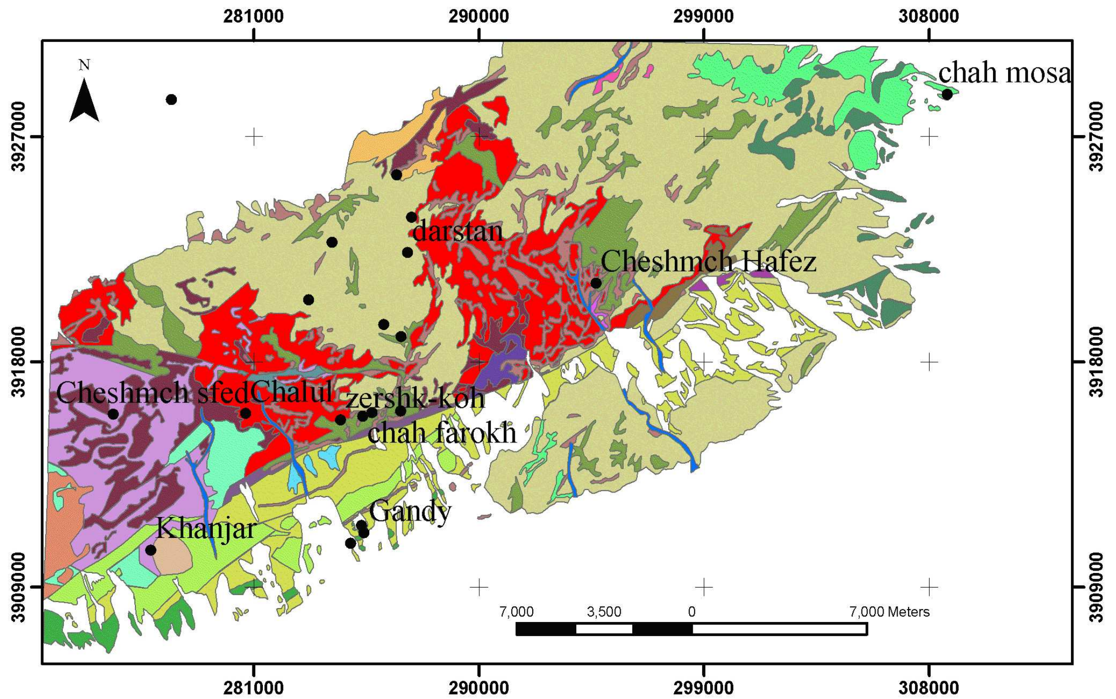

	ela	latite to andesitic lavas
	Epyc	Pyroclastic rocks
	Esp	Spilitic basalt
	Ets	Association of tuff and tufit
	Evbr	Red to grey volcanic breccias and miner tuffaceous sandstones
	Eba	Basalt, andesite-basalt, spilitic basalt
	El	Lenses of bioclastic nummulitic limestones
	Etr	Massive trachyandesite,trachyandesite basalt, miner andesitic dacite rocks
	Etv	Intermediate to basic submarine lavas and volcaniclastic rocks
	Klsh	Green shale, limestone, sandy limestone, miner sandstone
	Ksc	Sandstone and conglomerate
	Pzs	Grey to dark grey schist, miner green schist
	Rhyolite-rhyodac	Rhyolite-rhyodacitic tuff and tuffit, bentonite bearing
	Sk	Skarn
	dacit	Altered dacite and dacitic- andesite rocks
	dp	Quartz trachyandesite, trachyandesite, quartz latite
	eal	altered rocks
	epyc	Pyoclastic rocks, agglomerate and conglomerate
	et	Light green and cream rhyolitic tuff
	my	Catalastic metamorphosed rocks
	pzld	Thick bedded to massive metamorphosed dolomite and limestone
	qd	Quartz diorite, quartz monzodiorite
	qpi	Poorly consolidated, poorly sorted conglomerate
	qt	terraces

Figure 2. Generalized geological map of study area. Mineralized zones are outlined in dark. Dark circles are locations of gold and base metal deposits.

3.2. Faults/fractures map

In the study area, faults/fractures can influence localisation of stream sediment anomalies because (a) such geological features are common loci of epithermal Au deposits, whose element contents find their way into streams due to weathering and erosion and (b) the presence of such geological features indicates enhanced structural permeability of rocks in the subsurface, which facilitates upward migration of ground waters that have come in contact with and have leached substances from buried deposits. These arguments suggest that the significance of multi-element stream sediment anomalies in sample catchment basins can be screened or examined further by using fault/fracture density as a factor [10]. Figure 3, shows a map of faults/fractures in the study area, indicating that the epithermal Au deposits are localised mostly along certain north-northwest-trending faults/fractures. A fault/fracture density map can be created by calculating, per sample catchment basin, the ratio of number of pixels representing faults/fractures

in a sample catchment basin to number of pixels in that sample catchment basin. Most of the epithermal Au deposit occurrences in the study area are situated in sample catchment basins with moderate to high fault/fracture density (Figure 3).
Using the geological map of Moalleman area and investigating the trends of the faults in the area, we digitized the linear geological structures related to gold, lead and zinc mineralization. Figure 3 indicates the map of the faults and gold mineralization in the area.

3.3. Alteration, aeromagnetic and lithogeochemical maps.

We used combination band ratios (band5/band7, band4/band5, and band1/bandt3) of Landsat ETM+ satellite images data as a set representing hydrothermal alteration intensity evidence for modeling prospectivity for epithermal Au and base metal deposits in the Torud-Chah Shiran area (Figure 4).

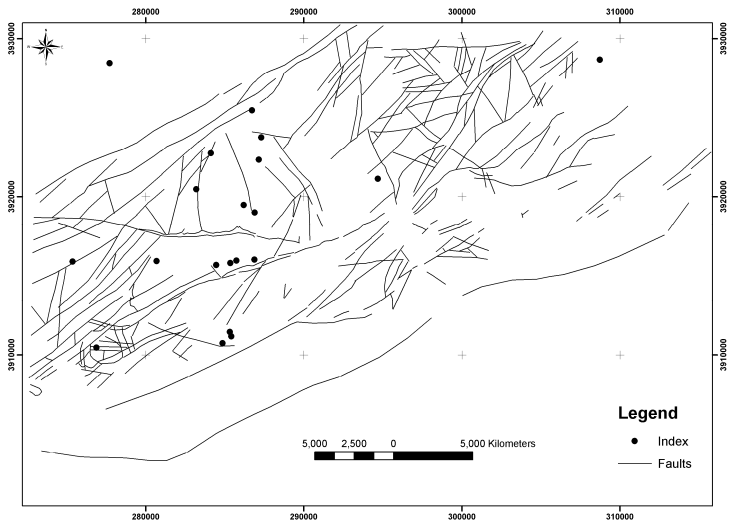

Figure 3. Map of faults/fractures in the stady are, compiled mostly from unpublished literature, geological and geophysical map.

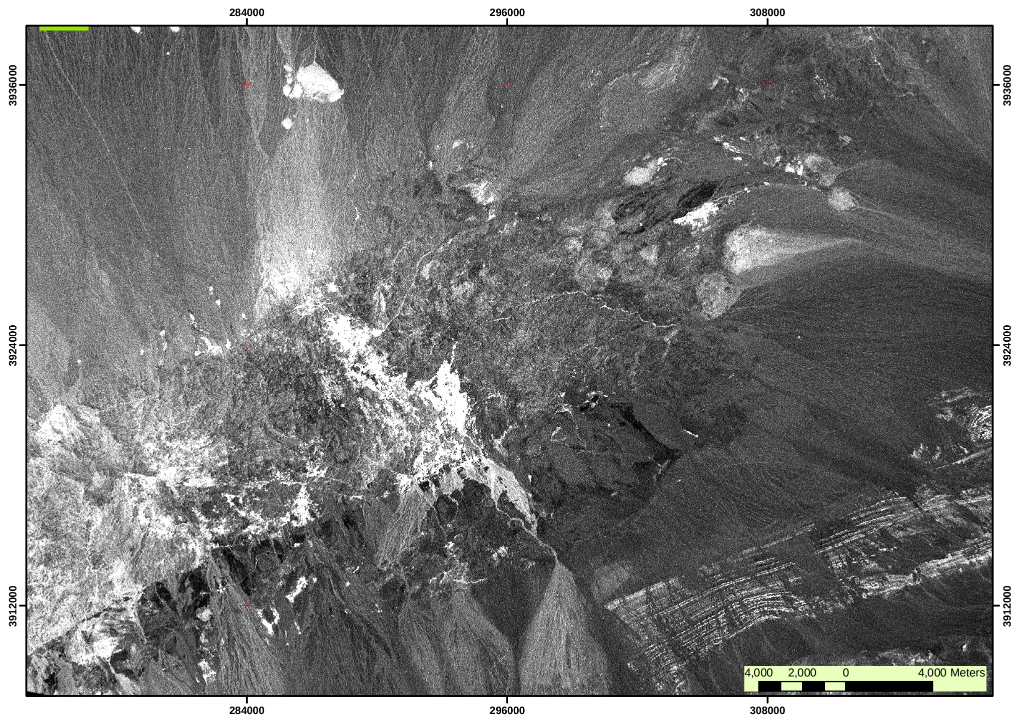

Figure 4. The hydrothermal alteration zones generates from the combinations selected Landsat ETM+ satellite images band ratios (5/7, 4/5, 1/3)

In this research work, the aeromagnetic map provided by the Geological Survey of Iran, was used for combination with other exploration maps. The aeromagnetic map was obtained following an airborne survey, carried out by Aeroservice Company, with flight lines spaced 7.5 km and constant altitude. It should be mentioned that other aeromagnetic maps with higher qualities, have also been provided that unfortunately, do not cover the whole study area, and are merely used for reviewing of geophysical data. Figure 4 shows the airborne magnetic map of the Moalleman area. As seen from this Figure, Gandi Au deposit is located in the vicinity of high total magnetic zones.

3. Fuzzy logic method

The fuzzy logic approach, which is considered to be one of the knowledge-driven methods, can be effective as a method to weight and combine spatial evidences when the proposition (such as "this location is favorable for mineral deposits") is vague [11]. Fuzzy logic uses membership functions (μ) and various different combination operators. Mathematically, a fuzzy set, A, is a set of ordered pairs:

$$A = \{(x, \mu_A(x)) \mid x \in X\},$$

where X= collection of objects, also known as the universal set and μ(x) = membership function or degree of compatibility of x in μ(x) (An, et al., 1991). The range of μ(x) is [0, 1], where 0 represents non-membership and 1 represents full membership. An, et al. (1991)

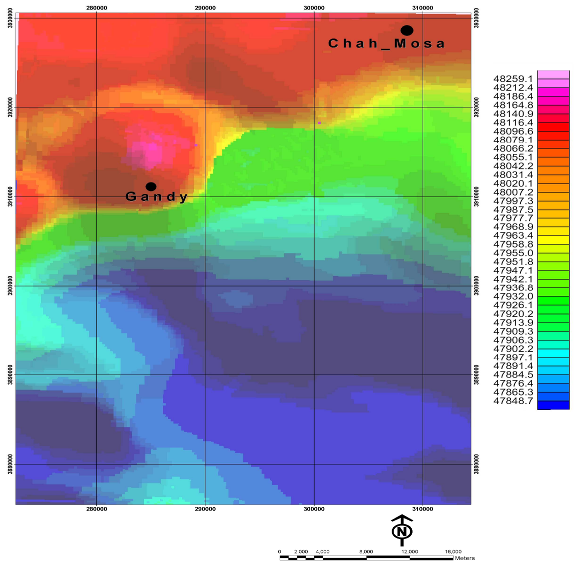

Figure 5. Geophysical data sets, residual total magnetic intensity (nT) (from Shuigen and Jianchang, 1996) used in the study.

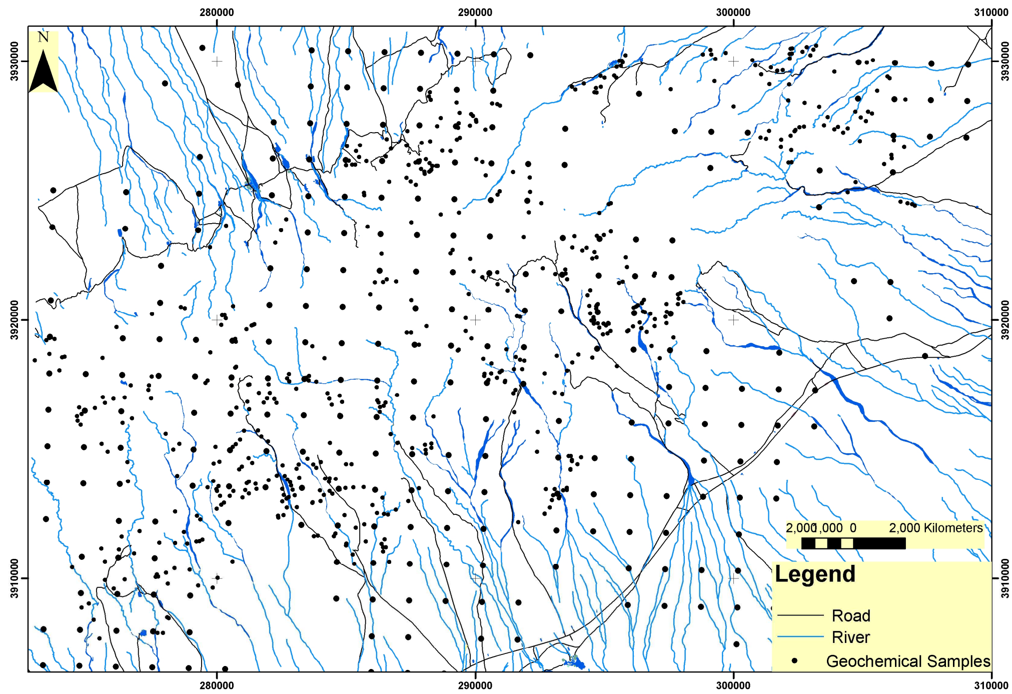

Figure 6. A map of spatial data of interest. Selection of spatial data by using attribute conditions is useful in analysis of geochemical data pertaining to different lithologies.

discussed five operators that were found to be useful for combining exploration datasets, namely the fuzzy AND, fuzzy OR, fuzzy algebraic product, fuzzy algebraic sum and fuzzy gamma operator. The fuzzy OR, for example, is like the Boolean OR (logical union) in that the output membership values are controlled by the maximum values of any of the input maps, for any particular location. Using this operator, the combined membership values are limited by the most suitable of the evidential map patterns. The OR-operator can be used where two map patterns represent the same level of evidence, and the combinations suggest evidence at higher probability. Gamma operator (γ) is a combination of the fuzzy algebraic product and the fuzzy algebraic sum, and produces output values that ensure a flexible compromise between the increasing tendencies of the fuzzy algebraic sum and the decreasing effects of the fuzzy algebraic product. Bonham-Carter [12], An et al. [13] and Cheng and Agterberg [14] presented additional information on the fuzzy operators for combining geological data.

Figure 7 shows three parallel networks that sequentially combine collateral fuzzy evidential maps transmitted by the fuzzifier through the fuzzy OR and fuzzy AND operators to yield three intermediate fuzzy evidential maps in the first stage, which are combined in the second stage using the fuzzy γ operator to generate the synthesized fuzzy favorability map. The maps that more likely to be conditionally-dependent were combined in the first stage of the inference engine using the fuzzy AND and the fuzzy OR operators. The choice of the fuzzy AND operator or the fuzzy OR operator in the parallel networks described above depended upon whether the presence of only one of the two fuzzy predictor maps to be combined was sufficient for the recognition of base-metal deposits in the province. The intermediate fuzzy predictor maps were combined in the second stage of the inference engine using the fuzzy operator γ with γ = 0.9, 0.83 and 0.93 to produce the three synthesized fuzzy favorability map. The map using γ=0.9 was selected since the threshold combined fuzzy favorability value narrows down the search area more judiciously in this map. The resulting binary favorability map is shown in Figure 8.

3.1 Model validation

The fuzzy logic (knowledge-driven) model was validated by overlaying the locations of known mineral deposits which are different from training data on the binary favorability map. Figure 8 showing the binary favorability map in which the high favorability areas, where occupy 14% of the study area that contain 83.4% of the known base-metal deposits.

4. Weights of evidence method

Weight of evidence (WofE) method is a quantitative method that uses a log-linear formulation of Bayes' rule of probability with an assumption of conditional independence to combine map patterns. WofE has been used by geologists to identify areas favorable for geologic

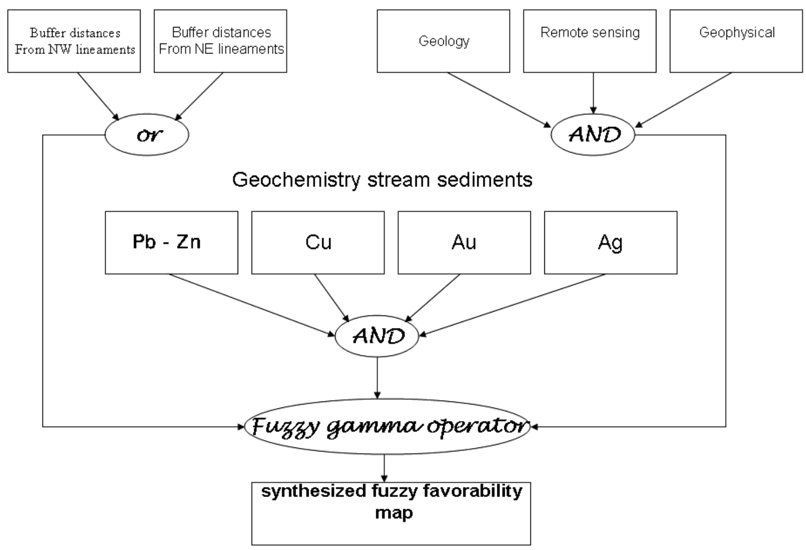

Figure 7. Generating synthesized fuzzy favorability map in Figure 8.

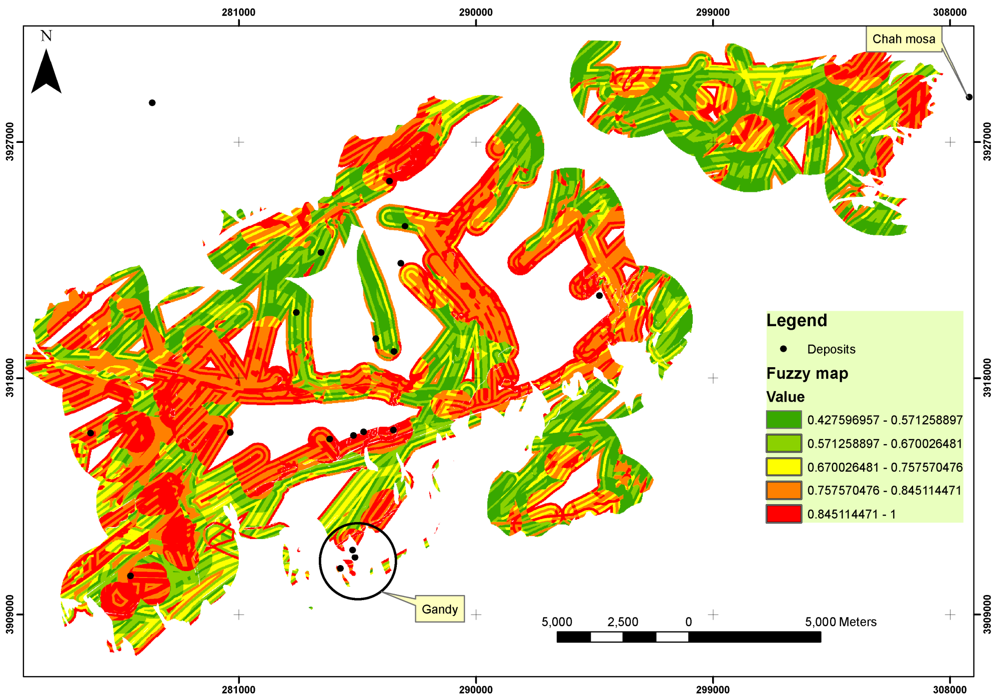

Figure 8. Potential map generated by fuzzy logic method

phenomena, such as mineralisation and seismicity. The WofE method allows one to explore the spatial relationship between known mineral deposits and exploration data sets from a variety of sources (Bonham-Carter 1994). In mineral exploration applications, a series of evidence maps (evidential themes) derived from geochemical, geophysical and geological data sets are combined to produce a mineral prospectivity (or potential) map. The spatial association of each evidential theme is assessed with respect to the locations of known deposits, used as training points. Because most studies of this type have only a limited number of deposits, it is advantageous to generalise the maps to a small number of classes, often to binary classes, because a weight is estimated for each class and these estimates are not robust when the number of training points is small. A pair of weights, W+ and W-, determined from the degree of overlap between the known deposits and the binary evidence map (e.g. geochemical anomaly map), is calculated for each map to be used as evidence. If there is no spatial association between the training points and the binary evidence map, then W+ = W- = 0. A positive W+ value indicates a positive association between training points and the evidence map. In this case, more of the known deposits occur on the map class than would be expected if the number of deposits occurring there could be explained as due to chance. Conversely, a negative association implies the occurrence of fewer known deposits on that map class than would be expected due to chance. The contrast value C, where C = W+ - W- , is a summary value that reflects the degree of spatial association between the evidence map and the mineral prospects (Table 1). The larger the C value, the greater is the spatial association. A study of weights and contrast values can facilitate the process of identifying breaks between background and anomalous values in geochemical data, or in identifying critical distances on evidential themes related to proximity to spatial objects [12]. The process of evaluating weights, contrast and reclassifications gives invaluable insight into the spatial associations present in the data (e.g. separation of background from anomaly in geochemistry, selection of optimal distances for buffering linear features, etc.). The effects of various sources of uncertainty on the final result can be modeled, such as the variances of weights and the variance due to missing data (incomplete surveys). A recent development allows the effect of kriging variance on the weights to be modeled [14]. The principal disadvantage of WofE method is that it assumes conditional independence between the data (evidence maps) (e.g. an elevated concentration in Au is independent of an elevated concentration in Zn, conditional on the locations of deposits). This conditional independence assumption is often violated when producing a prospectivity map, although the degree of violation depends on the choice and number of maps used as predictors.

One consideration with the WofE approach is the issue of conditional independence between the evidence maps. The nine binary maps were used to model mineral favorability but statistical tests showed some disagreement with conditional dependence, and thus, a recombination of the maps by factors was applied. Therefore, some evidence maps were combined resulting in four factor maps: geological factor, structural factor, geochemical factor, and geophysical factor. This favorability map is shown in Figure 9.

However, the omnibus test of conditional independence gives a value of 0.952 for the conditional independence ratio between the four factor maps, which still indicates conditional dependency amongst some of input predictor maps. This also suggests that values less than 0.85 may indicate a problem [12].

4.1 Model validation

The WofE (data-driven) model was validated by overlaying the locations of known mineral deposits on the binary favorability map (Figure 9) showing that in the binary favorability map, high favorability areas, which occupy 7.3% of the study area, contain 61.3% of the known base-metal deposits.

5. Comparison of fuzzy logic with weights of evidence results

To compare the results of fuzzy logic and WofE methods, map of differences obtained from the WofE and fuzzy logic modeling was prepared (Figure 10). The differences map was validated by overlaying the locations of known mineral deposits on the binary favorability map. Figure 9

Table 1(a). Summary statistics results for WofE analysis.

			Cu			
Class	Area_Sq_km	Points	C	S_C	stud_C_
Missing data	0.1738	1	0.0000	0.0000	0.0000
1(< 70%)	134.3838	18	3.3759	0.7529	4.4840
0(> 70%)	378.1939	2	-3.3646	0.7528	-4.4693
		Ag			
Missing data	0.1738	1	0.0000	0.0000	0.0000
1(< 70%)	59.7538	6	1.2482	0.5088	2.4532
0(> 70%)	452.8239	14	-1.2482	0.5088	-2.4532
		pb			
Class	Area_Sq_km	Points	C	s_C_	stud_C_
Missing data	0.1738	1	0.0000	0.0000	0.0000
1(< 70%)	110.6232	14	2.2540	0.5009	4.4996
0(> 70%)	401.9546	6	-2.2540	0.5009	-4.4996
		Zn			
Class	Area_Sq_km	Points	C	s_C_	stud_C_
Missing data	0.1738	1	0.0000	0.0000	0.0000
1(< 70%)	47.6618	4	0.9365	0.5809	1.6122
0(> 70%)	464.9160	16	-0.9365	0.5809	-1.6122
		Au			
Class	Area_Sq_km	Points	C	s_C_	stud_C_
Missing data	0.1738	1	0.0000	0.0000	0.0000
1(< 70%)	102.1085	14	2.3738	0.5019	4.7295
0(> 70%)	410.4693	6	-2.3601	0.5018	-4.7032

Area_Sq_km: area, measured in square km, Points: number of training points occurring in that condition, C: Contrast, s-C: standard deviation, stud_C: Studentized Contrast, which is the contrast, divided its standard deviation, a measure of spatial association between the deposits and the geochemical anomaly.

Table 1(b). Summary statistics results for WofE analysis.

	geophysics				
Class (intensity)	Area_Sq_km	Points	C	s_C_	stud_C_
40%>	313.8778308	2	-0.236769	0.7458348	-0.317455
70%>	95.5067964	2	1.0570945	0.7508131	1.4079328
90%>	186.7877957	4	1.1556289	0.5609841	2.0600031
80%>	421.6935264	13	2.1873892	0.4525707	4.8332537
	faults				
Class (Buffer)	Area_Sq_km	Points	C	s_C_	stud_C_
100 m	86.0525	4	-0.0808	0.5983	-0.1350
200 m	73.3935	1	-1.5312	1.0440	-1.4667
300 m	58.4778	4	0.4632	0.6030	0.7682
400 m	47.0714	1	-0.9705	1.0475	-0.9265
500 m	39.9143	5	1.2928	0.5766	2.2420
	geology				
Class	Area_Sq_km	Points	C	s_C_	stud_C_
Dacit	14.4990	5	2.3924	0.6261	3.8215
Eal	2.7476	1	2.0458	1.2501	1.6366
R-r	2.7927	1	2.0458	1.2501	1.6366
Klsh	16.3568	2	0.8070	0.7987	1.0103
Esp	17.2571	2	0.7340	0.7957	0.9224
	alterations				
Class (Buffer)	Area_Sq_km	Points	C	s_C_	stud_C_
500 m	83.4039	13	1.4765	0.4900	3.0131
1000 m	63.3741	2	-1.1490	0.7601	-1.5118
1500 m	58.5021	5	0.1109	0.5392	0.2057
2000 m	50.1777	0	0.0000	0.0000	0.0000

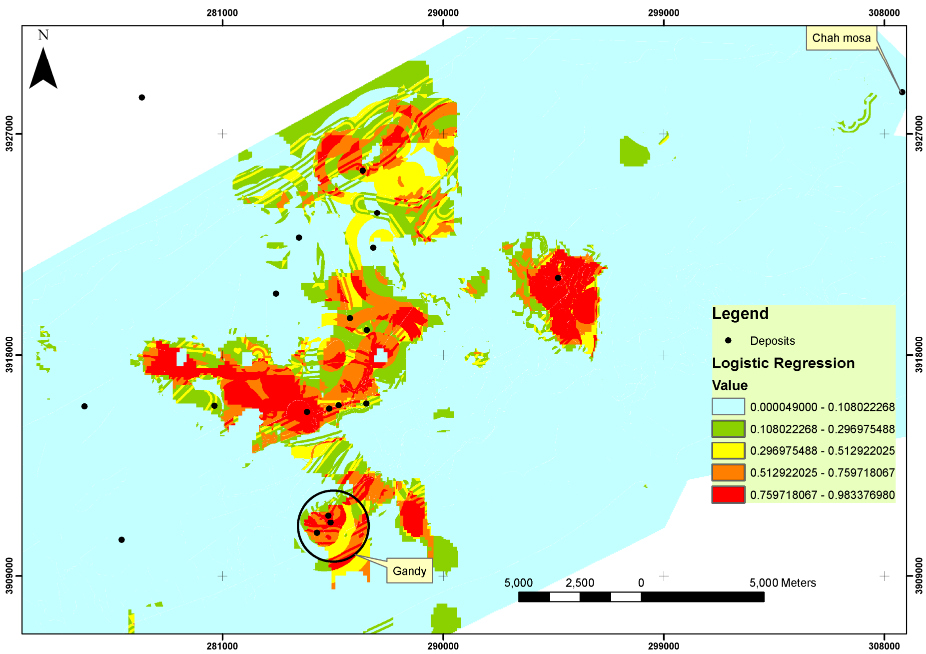

Figure 9. Potential map generated by logistic regression method.

shows that in the binary favorability map, high favorability areas, which occupy 5.5% of the study area, contain 72.2% of the known base-metal deposits.

5. Comparison of fuzzy logic with weights of evidence results

To compare the results of fuzzy logic and WofE methods, map of differences obtained from the WofE and fuzzy logic modeling was prepared (Figure 10). The differences map was validated by overlaying the locations of known mineral deposits on the binary favorability map. Figure 9 shows that in the binary favorability map, high favorability areas, which occupy 5.5% of the study area, contain 72.2% of the known base-metal deposits.

As can be seen from Table 2, the values in the difference map for high favorability area are reduced. Similarly, the confidence values show that difference map is reliable for mineral exploration in the study area.

6. Conclusions

A major benefit of WofE is the unbiased statistically derived weights it provides for individual layers of data. However, WofE is perceived by many users as both an oversimplification, due to its typically binary input, and yet overlay complex in mathematics. Multi-class WofE offers better representation of data distribution, but statistical noise can sometimes limit the effectiveness of multi-class weights. For example, potential maps generated from logistic regression method are not robust when the number of training points is limited.

Fuzzy logic methods offer gradational weighting schemes for individual data layers and relatively simple arithmetic operations for combining evidence layers into predictive models. With fuzzy logic, when data layers are assembled, it is carried out rom an expert's point of view. Expert input ensures the appropriate use of data, but the advantages of unbiased statistical weighting are diminished.

To provide a robust map of results, the maps were compared with each other and as a result, a map of rank differences was obtained. Finally, the results were tested by real field information, thus, the differences map was more fitted to the existing ground reality.

Acknowledgements

This paper was financially supported by a grant from Shahrood University of Technology. Also, we wish to thank the staff of the Geological Survey of Iran (GSI), especially Mr. M. Badakhshan and Mr. B. Firozi for providing us with the geological maps of the study area.

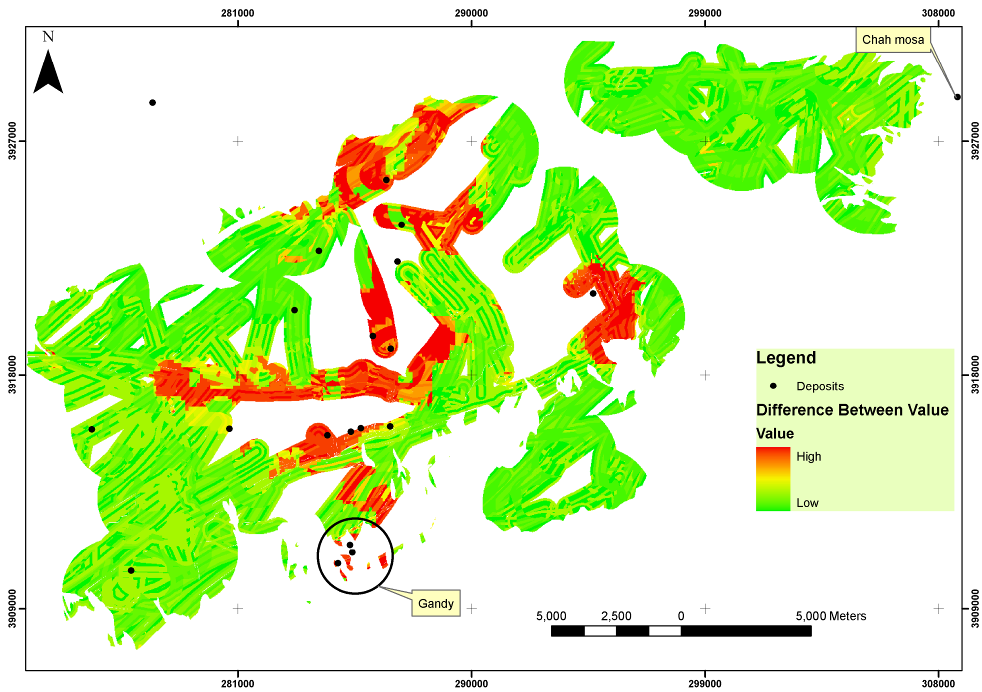

Figure 10. Map of rank differences comparing results obtained from the weights of evidence and fuzzy logic modeling.

Table 2. Percentage of confidences from generated maps.

Name	High favorability areas	Validation	Confidence
Knowledge-driven map	14%	83.4%	84%
Data-driven map	7.3%	61.3%	88%
Deference map	5.5%	72.2%	93%

References

[1]. Bonham-Carter, G.F., (1996). Geographic information system for geoscientists: modeling with GIS. Computer Methods in the Geosciences, 13, Pergamon, 398p.

[2]. Porwal, A., Carranza, E.J.M. and Hale, M., (2003). Knowledge-driven and data-driven Fuzzy models for predictive mineral potential mapping. Natural Resource Res. 12(1), 1-25.

[3]. Agterberg, F.P. and Cheng, Q, (2002). Conditional independence test for weights-of-evidence modeling. Natural Resource Res.11, 249-255.

[4]. Carranza, E.J.M., (2004). Weights-of-evidence modelling of mineral potential: a case study using small number of prospects, Abra, Philippines. Natural Resource Res. 13(3): pp. 173-187.

[5]. Asadi, H. H. and Hale, M., (2001). A predictive GIS model for mapping potential gold and base metal mineralization in Takab area, Iran. Computers & Geosciences, Vol.27. pp. 901-912.

[6]. Geological Survey of Iran. (2007). Geological map of Mo'aleman (Scale 1:100,000).

[7]. Safonav, Yu.G. (1997). Hydrothermal gold deposits: distribution, geological genetic types, and productivity of ore-forming systems. Geol. Ore Deposits 39, 20–32.

[8]. Shamanian, G.H., Hedenquist, J.W., Hattori, K.H. and Hassanzadeh, J. (2004). The Gandy and Abolhassani epithermal prospects in the Alborz magmatic arc, Semnan Province, Northern Iran: Economic Geol., 99, 691-712.

[9]. Shuigen, X. and Jianchang, Z. (1996). Explanatory Text of Geochemical Map of Mo'aleman. Geophysical and Geochemical Exploration Co., Jiangxi, China. Report No. 23. (Jointed Groups, The project has presented to the Ministry of Mines and Metals and Geological survey of Islamic Republic of Iran).

[10]. Carranza, E.J.M. and Hale, M. (1997). A catchment basin approach to the analysis of geochemical, geological data from Albay province, Philippines, J Geochem. Explor., 60(2):157-171.

[11]. Carranza, E.J.M., Hale, M. and Faassen, C. (2008). Selection of coherent deposit-type locations and their application in data-driven mineral prospectivity mapping. Ore Geol. Reviews 33(3-4): 536-558.

[12]. Bonham-Carter, G.F. (1994). Geographic Information Systems for Geoscientists: Modelling with GIS. Elsevier, 398 p.

[13]. An, P., Moon, W. M. and Rencz, A. (1991). Application of fuzzy set theory for integration of geological, geophysical and remote sensing data. Canadian J Explor. Geophysics, No. 27, 1-11.

[14]. Cheng, Q. and Agterberg, F. P. (1999). Fuzzy weights of evidence and its application in mineral potential mapping: Natural Resources Research 8, 27–35.